Structure and decomposition of [HFe(CO)₄(B₂H₅)], a revised behavior of an old uncharacterized complex

Abdeladim Guermoune [a], Driss Cherqaoui [a], Abdellah Jarid [a,*], Joel F. Liebman [b,*]

[a] Département de Chimie, Faculté des Sciences Semlalia, Université Cadi Ayyad, B.P. 2390, Marrakech, Morocco
[b] Department of Chemistry and Biochemistry, University of Maryland, Baltimore County, 1000 Hilltop Circle, Baltimore, MD 21250, USA

A B S T R A C T

The protonation reaction of the anionic complex [Fe(CO)₄B₂H₅]− gives a product which decomposes easily at −120 °C yielding [Fe(CO)₅] and B₂H₆ as reported by Coffy and Shore (J. Organomet. Chem. C27 (1990) 7394). In this work we have theoretically revised the understanding of this protonation using B3PW91/6-311+G** and B3P86/6-311+G** levels of theory. We found an unusual mode of coordination of B₂H₆ to the iron centre. The most stable structure exhibits a Fe−(μ-H)−B−(μ-H)−B five-membered ring which undergoes an isomerisation leading to the intermediate which displays an unusual interaction between [Fe(CO)₄] and B₂H₆ via (μ₃-H) binding. Atom-in-molecule (AIM) theory data indicate the presence of weak interactions between iron and boron atoms which are partially responsible of the facile decomposition of the formed complex. We consider that the decomposition pathway can occur in two steps; the first one gives [Fe(CO)₄] and B₂H₆ (the aim of this work) followed by second one where [Fe(CO)₄] undergoes a transformation to give [Fe(CO)₅], this step remaining ambiguous up to today. Parameters such as solvent effect, solvent interaction and spin split were considered to provide with reliable results about decomposition mechanism.

© 2010 Elsevier B.V. All rights reserved.

1. Introduction

Although it has been a significant development since the 1980s, the chemistry of metalloboranes $L_nM_mB_xH_y$ (L = organic ligand, M = metal, m = 1, 2) continues to be a source of innovations in structures and properties. This is due to the easy synthesis of such compounds, the abundant characterization means and hardware and software computational developments. If we restrict only to structural properties, the works of Shore [1–6] Kodama [7–9], Fehlner [3a,10–13], Shimoi [14–20], and their collaborators have greatly enriched the literature with valuable data that was so much needed in this area. However the borane ligand B_xH_y has several ways to be part of the coordination sphere of the metal. Formally, it can coordinate by the mono, di, tri,... hapto modes. It has been noticed that the symmetry of the borane ligand is always observed with regard to the metal centre. This means that the ligand keeps its structural identity by linking with the metal directly via the boron atoms or using B−H−M bridged bound. There are some reported binuclear complexes where the borane ligand loses its symmetry using both M−B and B−H−M linking motifs. Hence B_2H_5 in the complexes [Fe₂(CO)₆B₂H₅]− [3b] and [(CpRu)₂(η⁴-B₂H₅)(μ-

H)₅PMe₂] [6] adopts the mixed tetradentate mode. In the first both B−M and B−H−M bridged bonding are used with both metals whereas in the second B_2H_5 two M−B binding with one metal and B−H−M with the other Ru atom. In this later, B_2H_5 is parallel oriented to the Ru−Ru axis while a thermolysis at 60 °C shift it perpendicular to this axis being identically coordinated to both metals and featuring a mixed mode. This reorientation is accompanied by a B → B′ H migration. Similarly, B_2H_6 and B_3H_7 in Cd₂Rh₂B₂H₆ and nido-1,2(CpRu)₂(μ-H)B₃H₇ respectively [11] connect with the metal exhibiting a mixed mode. Nevertheless, at our knowledge there are no monometallic complexes have been reported featuring such behavior of the borane ligand.

On the other hand, since its discovery by Poliakoff and Turner [21] more than 30 years ago, [Fe(CO)₄] and its spin multiplicity has been the continuing subject of numerous studies [22–36] (The metal carbonyl is denoted in our paper by **4** to explicitly denote the number of CO groups, cf. **¹4** = Fe(CO)₄ singlet and **³4** = Fe(CO)₄ triplet). Although theory early showed that the C_{2v} triplet ground state **³4** (³B₂) is energetically slightly favoured over the singlet [23–26], the multiplicity behavior of Fe(CO)₄ in different reaction environments is still a subject of controversy. It was shown that **³4** could be converted to **¹4**·L (L = Xe, CH₄) by the photolysis of [Fe(CO)₅] in low temperature matrixes according to the reaction

* Corresponding authors. Tel.: +212 6 69 93 26 06.
E-mail addresses: jarid@ucam.ac.ma (A. Jarid), jliebman@umbc.edu (J.F. Liebman).

^{3}**4** + L → ^{1}**4** L, the reverse pathway could be brought about with low activation energies [27–30]. Nevertheless this suggestion did not receive complete agreement [31] since numerous studies suggested that the interaction of ^{1}**4** with the solvent (benzene, cyclohexane, heptanes) stabilizes the derived complex to be lower than ^{3}**4**, with no evidence for the uncomplexed singlet state ^{1}**4** [23–35]. In gas phase a singlet pathway is expected including the formation of the intermediate [Fe(CO)$_4$] via dissociation of an excited singlet state [Fe(CO)$_5$] yielding the lowest ^{1}**4** (^{1}A$_1$) [36]. The same result has been noticed by ultrafast electron diffraction spectroscopy showing clearly that the elimination of CO from [Fe(CO)$_5$] leads to the major transient ^{1}**4** (^{1}A$_1$ state) [37]. Nonetheless, it was still unclear if [Fe(CO)$_4$] is formed initially into the triplet state or through relaxation via singlet states. However, some of the previous studies suggested that the fragmentation of [Fe(CO)$_5$] follows the triplet pathway [38,39], but the singlet pathway has also been suggested by others [36,37] with initial formation of a transient intermediate ^{1}**4** with a very short lifetime, followed by an intersystem crossing leading to ^{3}**4** (^{3}B$_2$).

This work is a structural revision of the old synthesized complex HFe(CO)$_4$(B$_2$H$_5$) [6] which undergoes a fast decomposition to B$_2$H$_6$ and [Fe(CO)$_5$]. Additionally, we clarify the coordination mode of diborane within this complex and the role played by the iron tetracarbonyl fragment [Fe(CO)$_4$] in the degradation pathway.

2. Computational detail

All calculations presented in this study were performed with the Gaussian 03 program package [40] using density functional theory (DFT). Two hybrid functionals were applied: the Becke three parameter exchange functional [41] in combination with the Perdew (P86) [42] one, and the Becke three parameter functional in combination with a non-local correlation functional of Perdew and Wang [43] (PW91). In both cases we employed the 6-311+G** basis set. The complexes were fully optimized on the total Potential Energy Surface (PES) without geometrical restrictions using the Berny analytical gradient method [44]. The nature of the stationary points has been characterized by performing Hessian matrix (second derivative of energy) diagonalization and the vibrational normal modes analysis. The zero-point energy (ZPE) corrections obtained from the vibrational calculations have been added to the total energies at both B3P86 and B3PW91 levels. Intrinsic reaction coordinate (IRC) [45] calculations have been also carried out in order to be sure that stationary points are connected correctly to each other via the corresponding transition state. The atomic charges have been evaluated for [Fe(CO)$_4$(B$_2$H$_5$)]− using Natural Bond Orbital analysis (NBO) [46] and the 6-311+G(3df,2p) basis set. The atom-in-molecule (AIM) analysis was performed with the AIM2000 package [47] in order to calculate the properties of bond critical points (BCPs). Solvent effects were taken into account by means of polarized continuum model calculations (PCM) [48], choosing dichloromethane ($\varepsilon = 8.93$) as solvent using standard options. We chose this species because it was used in the original synthesis of the studied complex [6]. The single point PCM was done at 298.15 K on the gas phase optimized geometries. The atomic radii for the PCM calculations were specified using the UFF keyword.

3. Results and discussion

3.1. Structural and energetic analysis of [HFe(CO)$_4$(B$_2$H$_5$)]

Shore and Coffy report the electrophilic addition of acid to metalladiborane anions [M(CO)$_4$(η^2-B$_2$H$_5$)]− (M = Fe, Ru, Os) to yield the neutral compounds HM(CO)$_4$(η^2-B$_2$H$_5$) [6]. Using NMR

analysis, these authors proposed a **C**-like structure (Fig. 1) for these ruthenium and osmium complexes wherein the metallic centre keeps the well known octahedral environment of the homoleptic M(CO)$_6$ but where two adjacent carbonyl groups in *cis*-positions are replaced by H and B$_2$H$_5$ fragments. For the iron complex, the structure has not been determined because of its instability since the product decomposes above 120 °C leading to B$_2$H$_6$ and [Fe(CO)$_5$]. We have thoroughly investigated the H$^+$−[Fe(CO)$_4$(B$_2$H$_5$)]− interaction. Since protonation of the organometallic is not a simple process [49], numerous approaches have also been taken into account including the protonation of the ligands. We suggest that the protonation in the first step yields the neutral HFe(CO)$_4$(B$_2$H$_5$) complex. This latter species then undergoes a decomposition to B$_2$H$_6$ and [Fe(CO)$_4$] moieties. Our computation of the total singlet PES of HFe(CO)$_4$(B$_2$H$_5$) shows that, unlike the usually dihapto-coordination mode (two B−H−M bridged bonds) of B$_2$H$_5$ to one metallic centre, the absolute minimum **A** (Table 1) is characterized by Fe−B^1 and Fe−(μ-H)−B^2 binding (Fig. 1, Scheme 1). This coordination fashion is unprecedented in metallaborane chemistry. The inserted proton H^a then migrates to a bridged position between boron and metallic atom. The distance $d_{Fe-H^a} = 1.56$ Å is slightly longer than Fe-terminal hydrogen bonds in **B** and **C** (Table 2) which are of 1.515 and 1.512 Å respectively. These values are in good agreement with the experimental Fe−(μ-H) and Fe−(terminal-H) bond lengths which are 1.56 Å [50] and 1.53 Å [51] respectively. One can see also **A** as a coordination between H$_3$B(μ-H)BH$_2$ (an experimentally unisolated isomer of B$_2$H$_6$ but plausibly an intermediate of BH$_3$ dimerization [52]) and [Fe(CO)$_4$] fragments where the borane involves a mixed linking mode using a terminal hydrogen H^a (of B^1) to build a bridged bond Fe−H^a−B^1 and a directly bonded B^2−Fe (Scheme 1). Nevertheless the B−B distance (1.907 Å) which is longer than the usual bridged B$_2$(μ-H)M (M = Ru) one (1.733−1.840) [13,16,20,53,54] in the complexed state, does not support this view. In the bimetallic species (C$_5$Me)$_2$Ta$_2$(μ-Br)$_2$(B$_2$H$_6$) [55], the B−B bond exhibits a close distance to ours (1.88 Å). It has been concluded that this parameter is not consistent with a strong B−B bond. The **B** and **C** isomers, where the inserted hydrogen is in *trans* and *cis* positions respectively, are energetically less stable than **A**. They are higher by 8 and 10 kcal/mol respectively (Table 1). Not unreasonably, no significant change was observed when taking into account the ZPE and the solvent effects (Table 1).

B and **C** can be described as [HFe(CO)$_4$(η^2-B$_2$H$_5$)], where the B$_2$H$_5$ ligand is bound to the metal via the conventional di-hapto mode of coordination. In these complexes the distance B−Fe bond length (2.29 Å) is longer than the experimentally reported value, 2.217 Å in [Fe(C$_5$H$_5$)(CO)$_2$(η^2-B$_2$H$_5$)] [5] complex. On the other hand, the B−B distance ($d_{B-B} = 1.78$ Å) in both structures is in good agreement with the experimental values in this complex and in [Mo(η^5-C$_5$H$_5$)$_2$H$_2$(η^2-B$_2$H$_5$)] (1.79 Å) [54] as well as in isolated B$_2$H$_6$ (1.76 Å) [56] whereas the Fe−B^2 bond length (2.19 Å, Table 2) is also close to the observed one in [Fe(C$_5$H$_5$)(CO)$_2$(η^2-B$_2$H$_5$)] (2.217 Å) [32].

We have performed the AIM [57] partitioning scheme to obtain more information about the variation in the electronic density of the complex **A** (Table 3, Fig. 2). Some AIM parameters that are important to describe the bonding nature of the studied systems are summarized in Table 3. This analysis shows that there are no bond critical points (BCP) between boron atoms and between Fe and B^1 atoms (Fig. 2). This means that there is no interaction between these atoms, whereas a ring critical point was localized which emphasizes a cyclic Fe−B^2−H^b−B^1−H^a framework (Fig. 2). According to the sign of the Laplacian, there are two main categories of the bonding interactions: i) $\nabla^2\rho_{BCP} < 0$ which indicates that the electronic charge is concentrated in the internuclear region

A

B

C

D

TS$_{AC}$

TS$_{BC}$

TS$_{AD}$

^{1}**4.solv**

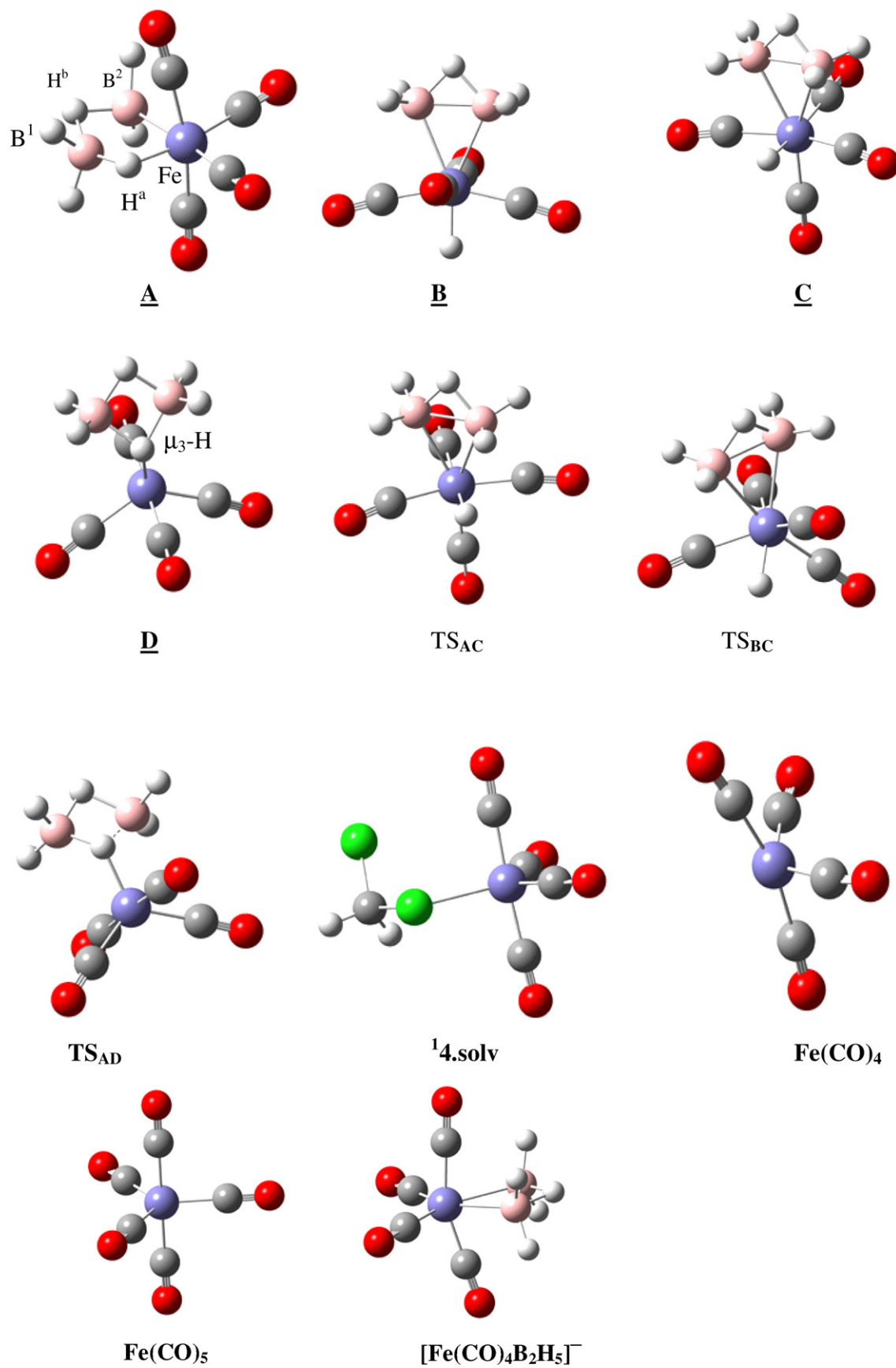**Fe(CO)$_4$**

Fe(CO)$_5$

[Fe(CO)$_4$B$_2$H$_5$]$^-$
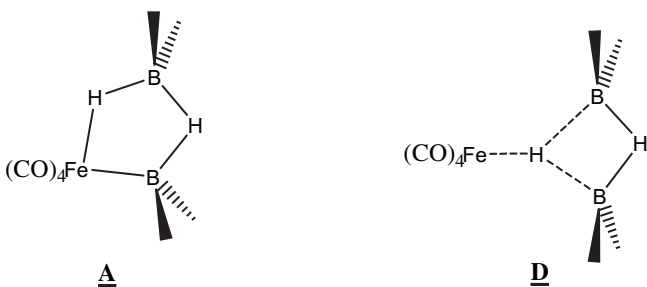
Fig. 1. Minima and TSs structures localized on the total PES.

Table 1

Relative B3P86/6-311+G** and B3PW91/6-311+G** energies ΔE, ΔE + ZPE, ΔE_s (with solvent effect) in kcal/mol of all minima and transition states of [HFe(CO)$_4$(B$_2$H$_5$)] total PES.

Structures	B3P86			B3PW91		
	ΔE	ΔE + ZPE	ΔE_S	ΔE	ΔE + ZPE	ΔE_S
A	0.0	0.0	0.0	0.00	0.0	0.0
B	7.5	7.3	7.8	7.5	7.3	7.8
C	9.9	9.8	10.1	10.0	9.8	10.1
D	14.1	14.2	15.2	14.2	14.2	15.3
	9.0	*7.9*	*6.8*	*7.1*	*5.9*	*4.7*
Fe(CO)$_4$ + B$_2$H$_6$	23.1	22.0	22.0	21.3	20.2	20.1
TSAC	10.9	10.5	11.1	10.9	10.6	11.1
TSAD	14.8	14.0	15.9	14.8	14.1	15.9
TSBC	24.2	23.3	25.5	24.3	23.5	24.6

Values in italics correspond to energy differences between Fe(CO)$_4$ + B$_2$H$_6$ and **D**. Total energy values of **A** are: $E(\mathbf{A})_{B3PW91} = -1770.26459$ a.u.; $E(\mathbf{A})$ + ZPE $_{B3PW91} = -1770.169069$ a.u.; $E_S(\mathbf{A})_{B3PW91} = -1770.26945$ a.u.

Table 2

Selective distances in Å of [HFe(CO)$_4$(B$_2$H$_5$)] optimized minima.

Structures	Fe–H^a	B^1–H^a	B–H^b	B^1–B^2	B^1–Fe	B^2–Fe
A	1.559	1.408	1.305/1.298	1.907	2.292	2.189
	1.563	*1.412*	*1.308/1.302*	*1.909*	*2.297*	*2.195*
B	Fe–H					
	1.504	–	1.305	1.783	2.258	2.258
	1.507	–	*1.308*	*1.787*	*2.264*	*2.264*
C	1.503	–	1.299	1.784	2.293	2.293
	1.506	–	*1.303*	*1.787*	*2.299*	*2.299*
D	Fe–(μ^3-H)	B–(μ^3-H)				
	1.648	1.373	1.319	1.856	2.535	2.535
	1.654	*1.376*	*1.322*	*1.859*	*2.543*	*2.543*

First row values from B3P86 and second row (italic) values from B3PW91 calculations.

as is the case of an electron-sharing (or covalent) interaction, and ii) $\nabla^2\rho_{BCP} > 0$ which indicates the electronic charge depletion along the bond as is the case in a closed-shell electrostatic interaction [57]. The first category concerns the typical covalent and the polar-covalent bonds, and the second one corresponds to the ionic and van der Waals interactions. Only Fe–B^2 and B^1–H^a bonds (Table 3) can be classified as covalent while the others can be considered as closed-shell interactions. The electronic energy density $H(r)$ at BCP is defined as $H(r) = G(r) + V(r)$, where $G(r)$ and $V(r)$ correspond to the kinetic and potential energy densities respectively [58]. The sign of $H(r)$ determines whether the charge accumulation, at a given point, is stabilizing ($H(r) < 0$) or destabilizing ($H(r) > 0$). The calculated values of $H(r)$ reported in Table 3 are negative for all bonds, which have a stabilizing effect due to the amassing charge in bond region supporting a covalent bond character. Therefore, since $\nabla^2\rho(r)$ is positive and $H(r)$ is negative, it can be concluded that these bonds characters are partially covalent and partially electrostatic. Taking into account this topological characterization of the Fe–H (B$_2$H$_5$) bonds, and the low binding character between major atoms forming the five-membered ring, we can advance that the complex **A** is strongly able to undergo some structural transformations.

Starting from **A**, **D** can be reached by moving slightly the bridged hydrogen H^a toward the ring centre. This complex is energetically 14 kcal/mol higher than **A** and exhibits an unusual structure with a hydrogen atom located between three heavy centres (μ$_3$-H, Fig. 1, Scheme 1). A similar example was reported recently in a (B$_2$H$_6$)-benzene study [59] wherein the benzene–diborane system was taken as a model to describe the nature of the observed interaction between an n-B$_{18}$H$_{22}$ cluster and benzene molecule [60]. Using the appropriate treatment at different levels of computational theory, this interaction has been found to be mostly dispersive with a stabilizing energy of 3.7 kcal/mol [58]. In our case, the interaction between (μ$_3$-H) and the iron centre is partially covalent and

partially electrostatic ($\nabla^2\rho(r) > 0$; $H(r) < 0$). Because of the low value of $H(r)$, the electrostatic character prevails. In contrast the (μ$_3$-H)–B bond is purely covalent ($\nabla^2\rho(r) < 0$). Let us remember that the (μ$_3$-H) structure has been reported also in the [{(Et$_2$C$_2$B$_4$H$_4$)FeH–(C$_5$Me$_4$)}$_2$C$_6$H$_4$] complex [61] where two boron atoms are bound to the iron centre. In this complex, the Fe–(μ$_3$-H) bond length (1.63 Å) is close to the analogous one in our **D** isomer (1.64 Å and 1.65 Å, Table 2). Nevertheless, the bond length Fe–B which is about 2.53 Å is higher than the observed longest one (2.36 Å) [51,62]. This does not support the existence of any interaction between iron and boron atoms in this structure. The same remark for B–B bond length (1.85 Å) which is in agreement with the absence of BCPs between these centres (Fig. 2). In fact, the isomer **D** can be viewed as a result of a weak interaction between B$_2$H$_6$ and [Fe(CO)$_4$] being the important isomeric form inducing the decomposition of the neutral [HFe(CO)$_4$B$_2$H$_5$] complex.

We have failed to reproduce all isomers of protonated complex in their triplet state. It is the reason we didn't make comparison between singlet and triplet total PES.

In order to extend this study to Os and Ru congener of the complex herein treated, the same structural analysis has been undertaken for these two complexes and the results seem to be similar to Fe ones except **A** for osmium and **D** for ruthenium which exhibit a slight geometric difference (Fig. 3). However for both [HM(CO)$_4$B$_2$H$_5$] (M = Ru, Os) the absolute minima adopt the **A**-like structure on the entire PES.

We have chosen LANL2TZ(f) [63]/6-311+G** level for Ru and Os complexes because it reproduces the same energy deviation regarding **A** for iron centre at B3PW91(B3P86)/6-311+G** methods (Table 4). Note that for both complexes, the structure **A** remains the absolute minimum, and the energy difference between the three isomers **A**, **B** and **C** are very slight suggesting easy isomerisation phenomenon with some low energy barriers between these structures. On the other hand, the structures **A** of iron and ruthenium complexes are geometrically close and exhibit the same coordination mode of the borane whereas the osmium one shows

Scheme 1.

Table 3

AIM Analysis, bond critical points (a.u.).

| Structures	Bond type	$\rho(r)$	$\nabla^2\rho(r)$	$G(r)$	$V(r)$	$H(r)$
A	Fe–B^2	0.072	−0.002	0.026	−0.053	−0.027
	Fe–H^a	0.108	0.222	0.099	−0.142	−0.043
	B^1–H^a	0.098	−0.070	0.056	−0.130	−0.074
	B^2–H^b	0.121	0.082	0.124	−0.227	−0.103
	B^1–H^b	0.122	0.043	0.116	−0.221	−0.105
D	(μ^3-H)–B	0.106	−0.011	0.082	−0.167	−0.085
	(μ^3-H)–Fe	0.080	0.254	0.087	−0.110	−0.023
	B–H^b	0.121	0.049	0.116	−0.220	−0.104
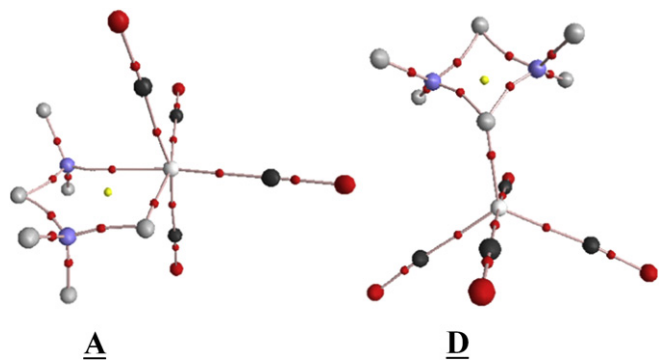
Fig. 2. AIM Molecular graphics for complexes **A** and **D**. Atoms are indicated by spheres, the bond critical points (BCPs) by red, and the ring critical points (RCPs) by yellow dots.

that H^a is so far from boron atoms. In fact, the B^1–H^a distance increases from the iron complex to osmium one (Table 5). Moreover, in the osmium complex the $\angle B^1MH^a$ (60.4°) angle has the higher value compared to ruthenium (40.7°) and iron (37.6°) complexes. This means that H^a is connected only to Os centre as supported by the AIM calculations (see Supporting material). On the other hand, the osmium complex **D** shows the highest energy deviation within the three complexes. This can explain why [HOs(CO)$_4$B$_2$H$_5$] decomposes slowly whereas in the Ru case this deviation is the lowest one. This suggests a faster decomposition unlike what has been reported [6]. Accordingly, we have performed an AIM calculation again to get more information about the bonding nature within these two complexes (see Supporting material). Apart from the linking nature, both complexes show the very close electronic energy density $H(r)$ which indicates the stability of the bond. All values are comparable and close each other for both complexes except for B^1–H^a. In fact, $H(r)$ is less stabilizing for the ruthenium complex. This means that the B^1–H^a bond in the iron complex is stronger than ruthenium one and the hydrogen atom is able to move straight to the B$_2$H$_5$ fragment to form **D** complex. This is probably the reason why the iron complex decomposes more rapidly than the osmium and ruthenium ones. In the next section we will investigate the kinetic behavior of decomposition of iron complex with complicity of other factors.

3.2. Rearrangement pathway and molecular stability

For a better understanding of the main interactions between the inserted proton H$^+$ and the anionic complex [Fe(CO)$_4$B$_2$H$_5$]$^-$ that are involved in the stability of these complexes, we have examined the distribution of the atomic charges using NBO analysis [46]. The localized negative charges on boron atoms and on equatorial
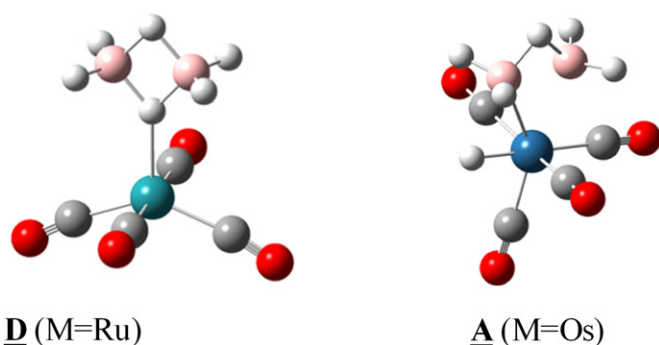
Fig. 3. Structures of **D** (Ru complex) and **A** (Os complex) with their slight differences from structures **A** and **D** of the homologous Fe complex.

Table 4
Relative B3PW91/LANL2TZ(f)/6-311+G** energies ΔE in kcal/mol of all minima for HM(CO)$_4$B$_2$H$_5$ (M = Os, Ru, Fe).

Structures	M = Fe	M = Ru	M = Os
A	0.00	0.00	0.0
C	10.0	5.9	3.1
B	7.4	3.9	5.9
D	15.2	13.6	29.4

carbons favour the proton approach on the metal from this side, to form the complex **A** (Fig. 1, see Supporting material). However, the *trans* position in [Fe(CO)$_4$B$_2$H$_5$]$^-$ seems to favour the proton insertion with a less bulky effect but the highly condensed negative charge on the boron atoms and terminal hydrogen might advantage the **C** formation.

Isomers **B** and **C** are higher in energy by 8 and 10 kcal/mol (Table 1) than **A** in the total PES of the [HFe(CO)$_4$(B$_2$H$_5$)] neutral structure. These complexes undergo an isomeric rearrangement leading to **A**. However, only 1 kcal/mol is needed to transform **C** to **A** in one step via a transition state **TS$_{AC}$**, but the reverse pathway costs about 11 kcal/mol. On the other hand, in spite of its stability than **C**, the *trans*-conformer **B** needs two steps to be transformed to **A**. The first one needs 17 kcal/mol as activation energy to go beyond **TS$_{BC}$** toward **C**, followed by the second step **C** → **A**.

On the other hand, as we have cited in the last section, **D** can be obtained by moving the bridged hydrogen within **A** toward the middle B–B bond. This transformation takes place via a transition state **TS$_{AD}$**. This latter shows the Fe–B^2 bond breaking (2.363 and 2.369 Å at B3P86 and B3PW91 respectively) and the beginning of the formation of B^2–H^a bond (1.56 Å). It is also interesting to note that the Fe–H bond lengthening in the direction **A** → **TS$_{AD}$** → **D** (1.56, 1.61, 1.65 Å) is consistent with the formation of B$_2$H$_6$ within **D**. Taking into account the B–(μ_3-H) (1.37 Å) and the B–B (1.85 Å) bond lengths which are slightly longer than the experimental ones [64] (1.31 and 1.776 Å respectively), we can consider **D** as an activated complex leading to the B$_2$H$_6$ and [Fe(CO)$_4$] liberation. This complex constitutes the first example involving interaction between B$_2$H$_6$ and iron tetracarbonyl. We note that the B3P86 and B3PW91 structures of [Fe(CO)$_4$] are in good agreement with the characterized one by ultrafast electron diffraction [37]. **A** → **D** transformation requires about 15 kcal/mol as activation energy but the reverse pathway occurs easily with less than 1 kcal/mol. Furthermore the complex **D** seems to be more stable than the decomposition products (B$_2$H$_6$ and [Fe(CO)$_4$]) by about 9 and 7 kcal/mol at B3P86 and B3PW91 respectively (Table 1). While taking into

Table 5
Selected bond lengths (Å) of [HM(CO)$_4$(B$_2$H$_5$)] (M = Fe, Ru, Os) optimized minima.

Structures	M–H^a	B^1–H^a	B–H^b	B^1–B^2	B^1–M	B^2–M
A	1.556	1.421	1.309/1.301	1.907	2.291	2.195
	1.665	*1.561*	*1.323/1.289*	*1.889*	*2.385*	*2. 318*
	(1.666)	(2.126)	(1.319/1.292)	(1.811)	(2.379)	(2.390)
B	M–H					
	1.500	–	1.308	1.788	2.258	2.265
	1.640	–	*1.308*	*1.781*	*2.407*	*2.407*
	(1.665)	–	(1.308)	(1.802)	(2.398)	(2.398)
C	1.502	–	1.302	1.786	2.300	2.300
	1.622	–	*1.303*	*1.773*	*2.419*	*2.419*
	(1.659)	–	(1.302)	(1.777)	(2.430)	(2.430)
D	M–(μ_3-H)	B–(μ_3-H)				
	1.644	1.381	1.322	1.863	2.521	2.521
	2.058	*1.350*	*1.318*	*1.787*	*3.201*	*3.201*
	(1.771)	(1.419)	(1.326)	(1.925)	(2.589)	(2.589)

Values in normal font are for M = Fe, in italics for M = Ru and in parentheses are for M = Os.

account the ZPE correction, this barrier decreases by about 1 kcal/mol and by about 2 kcal/mol when the solvent effect is taken into account (Table 1). Only 4.7 and 6.8 kcal/mol at B3PW91 and B3P86 respectively are needed for the **D** decomposition leading to B_2H_6 and [Fe(CO)$_4$]. This low barrier can be ensured by intra or inter-molecular interactions or by the medium effects and explains why the complex undergoes a fragmentation at low temperatures.

$$Fe(CO)_4(B_2H_5) + H^+ \rightarrow \mathbf{A} \tag{1}$$

$$\Delta E_{B3PW91} = -312.0 \text{ kcal/mol}; \Delta E_{B3P86} = -311.3 \text{ kcal/mol}.$$

$$\mathbf{D} + H_2CCl_2 \rightarrow {}^1\mathbf{4} \cdot H_2CCl_2 + B_2H_6 \tag{2}$$
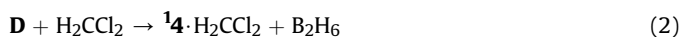
$$\Delta E_{B3PW91} = -3.8 \text{ kcal/mol}; \Delta E_{B3P86} = -3.8 \text{ kcal/mol}.$$

$$\mathbf{A} + CO \rightarrow Fe(CO)_5 + B_2H_6 \tag{3}$$

$$\Delta E_{B3PW91} = -22.3 \text{ kcal/mol}; \Delta E_{B3P86} = -22.3 \text{ kcal/mol}.$$

As in any reaction, the magnitude of the energy barrier has an important role in chemical reactivity both in terms of rate and yield. Hence, the released energy from reaction (1) can ensure easily all the interconversions from **B** up to the decomposition products. However, the released energy is overestimated in the gas phase relative to the condensed phase where the exothermicity of reaction (4) is about 6 kcal/mol. This protonation energy is more realistic and favours the formation of isomer **A** over that of **B** or **C**.

$$[Fe(CO)_4(B_2H_5)]^- + HCl \rightarrow \mathbf{A} + Cl^- \tag{4}$$
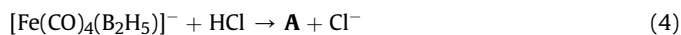
$$\Delta E_{B3PW91} = -5.9 \text{ kcal/mol}; \Delta E_{B3P86} = -5.9 \text{ kcal/mol}.$$

The H_2CCl_2 has a dual effect: weakening the [B_2H_6–Fe(CO)$_4$] interaction within **D** complex and pushing the diborane ligand to take the corresponding position in ${}^1\mathbf{4} \cdot H_2CCl_2$ (Figs. 1 and 3). This latter is about 4 kcal/mol lower than **D** (reaction (2)). It exhibits the well known coordination mode between chlorine atom and metallic centre via the interaction between the lone pair of the halogen atom and the vacant d orbitals of the metal centre. An additional interesting point is the possible [Fe(CO)$_4$] spin splitting on the process. However, the singlet state ${}^1\mathbf{4}$ is well known to be less stable than ${}^3\mathbf{4}$. This latter is close to **D** isomer ($\Delta E = -1.5$ and

1.3 kcal/mol at B3PW91 and B3P86 levels respectively). This spin change is exothermic and [Fe(CO)$_4$] in its triplet state become lower than ${}^1\mathbf{4}$ by 8.7 and 7.7 kcal/mol at B3PW91 and B3P86 respectively. This intersystem crossing, leading to the more stable triplet state, supports our mechanism of B_2H_6 release from the [HFe(CO)$_4$B$_2$H$_5$] complex while we consider the direct pathway $\mathbf{D} \rightarrow {}^3\mathbf{4} + B_2H_6$.

Taking all these results together, the reverse pathway to **A** still possible since this latter is the most stable on the total PES (Fig. 4). Nevertheless, if we consider [Fe(CO)$_5$] and B_2H_6 as final products of the decomposition as it was previously reported [6], it is clear that the complex **A** lies consistently higher by 22 kcal/mol (reaction (3)). The carbonylation of species ${}^3\mathbf{4}$, ${}^1\mathbf{4}$ and ${}^1\mathbf{4} \cdot H_2CCl_2$ is plausible and thereby generate [Fe(CO)$_5$]. Let us bear in mind that, up to now, the transformation from [Fe(CO)$_4$] and ${}^1\mathbf{4} \cdot L$ (L = solvent) to [Fe(CO)$_5$] remains mechanistically unclear − how does another [Fe(CO)$_4$] provide the additional CO?

4. Conclusion

In this contribution, we have revised structurally and mechanistically an old synthesized complex [HFe(CO)$_4$(B$_2$H$_5$)] using B3PW91/6-311+G** and B3P86/6-311+G** levels of theory. By exploring the total potential energy surface, we have shown that this complex exhibits new modes of coordination of the diboryl B_2H_5. However, the most stable structure is characterized by a mixed mode of coordination of B_2H_6 around the iron centre (Fe−H−B and Fe−B interactions). On the other hand, the B_2H_6 detachment process is characterized by a [Fe(CO)$_4$]−B$_2$H$_6$ weak interaction implying a (μ_3-H) triple connectivity of one bridged H of the diborane between the metal and both borons. According to AIM analysis, both structures are characterized by a weak connection of the diborane entity to iron centre explaining the facile decomposition of the complex. The first step of decomposition gives [Fe (CO)$_4$] + B_2H_6. Solvent effects and spin-state splitting in tetra-carbonyl-iron reduce the energy barrier of decomposition. The second step seems to involve a fifth carbonyl group (from a plausible decomposition of a [Fe(CO)$_4$] unit) leading to the observed [Fe (CO)$_5$] product. The Ru and Os homologous complexes have close behaviors except some critical points on their PES. The present work indicates that it is desirable to revise the [HFe(CO)$_4$(B$_2$H$_5$)] characterization using contemporary experimental techniques.

Appendix. Supporting material

Supplementary information associated with this article could be found on-line, at doi:10.1016/j.jorganchem.2010.03.021.

References

[1] F. Takusagawa, A. Fumagalli, T.F. Koetzle, S.G. Shore, T. Schmitkons, A. V. Fratini, K.W. Morse, C.-Y. Wei, R. Bau, J. Am. Chem. Soc. 103 (1981) 5165.
[2] M.A. Toft, J.B. Leach, F.L. Himpsl, S.G. Shore, Inorg. Chem. 21 (1982) 1952.
[3] (a) R.L. DeKock, P. Deshmukh, T.P. Fehlner, C.E. Housecroft, J.S. Plotkin, S. G. Shore, J. Am. Chem. Soc. 105 (1983) 815;
(b) G.B. Jacobsen, E.L. Andersen, C.E. Houscroft, F.-E. Hong, M.L. Buh, G.J. Long, T.P. Fehlner, Inorg. Chem. 26 (1987) 4040.
[4] S.K. Boocock, M.A. Toft, K.E. Inkrott, L.Y. Hsu, J.C. Huffman, K. Folting, S. G. Shore, Inorg. Chem. 23 (1984) 3084.
[5] T.J. Coffy, G. Medford, J. Plotkin, G.L. Long, J.H. Huffman, S.G. Shore, Organo-metallics 8 (1989) 2404.
[6] T.J. Coffy, S.G. Shore, J. Org. Chem. 394 (1990) C27.
[7] S.A. Snow, G. Kodama, Inorg. Chem. 24 (1985) 795.
[8] M. Kameda, G. Kodama, J. Am. Chem. Soc. 102 (1980) 3647.
[9] M. Kameda, G. Kodama, Inorg. Chem. 19 (1980) 2288.
[10] J. Feilong, T.P. Fehlner, A.L. Rheingold, J. Org. Chem. 348 (1988) C22.
[11] X. Lei, M. Shang, T.P. Fehlner, J. Am. Chem. Soc. 121 (1999) 1275.
[12] X. Lei, A.K. Bandyopadhyay, M. Shang, T.P. Fehlner, Organometallics 18 (1999) 2294.
[13] X. Lei, M. Shang, T.P. Fehlner, Chem. Eur. J. 6 (2000) 2653.
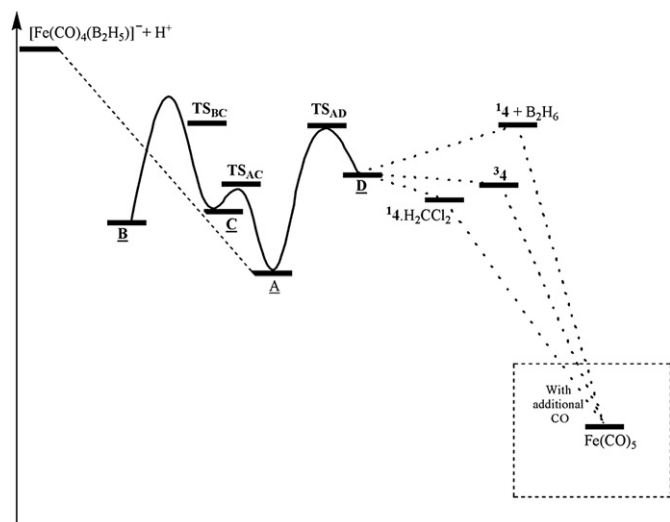[14] M. Shimoi, K. Katoh, T. Tobita, H. Ogino, Inorg. Chem. 29 (1990) 814.

Fig. 4. Energy profile of the protonation, isomerisation and fragmentation of the [Fe (CO)$_4$B$_2$H$_5$]− complex.

[15] K. Katoh, M. Shimoi, H. Ogino, Inorg. Chem. 31 (1992) 670.
[16] L.N. Pangan, Y. Kawano, M. Shimoi, Organometallics 19 (2000) 5575.
[17] L.N. Pangan, Y. Kawano, M. Shimoi, Inorg. Chem. 40 (2001) 1985.
[18] M. Shimoi, S. Ikubo, Y. Kawano, J. Am. Chem. Soc. 120 (1998) 4222.
[19] K. Katoh, M. Shimoi, H. Ogino, Inorg. Chem. 31 (1992) 670.
[20] M. Hata, Y. Kawano, M. Shimoi, Inorg. Chem. 37 (1998) 4482.
[21] M. Poliakoff, J.J. Turner, J. Chem. Soc., Dalton Trans. (1973) 1351.
[22] (a) M. Poliakoff, J.J. Turner, J. Chem. Soc., Dalton Trans. (1974) 2276;
     (b) T.J. Barton, R. Grinter, A.J. Thomson, B. Davies, M. Poliakoff, J. Chem. Soc., Chem. Commun. (1977) 841;
     (c) M. Poliakoff, E. Weitz, Acc. Chem. Res. 20 (1987) 408;
     (d) N. Leadbeater, Coord. Chem. Rev. 188 (1999) 35;
     (e) M. Poliakoff, J.J. Turner, J. Angew. Chem. Int. Ed. 40 (2001) 2809.
[23] J.K. Burdett, J. Chem. Soc., Faraday Trans. 2 70 (1974) 1599.
[24] M. Elian, R. Hoffmann, Inorg. Chem. 14 (1975) 1058.
[25] A. Veillard, Nouv. J. Chim. 5 (1981) 599.
[26] C. Daniel, M. Bernard, A. Dedieu, R. Wiest, A. Veillard, J. Phys. Chem. 88 (1984) 4805.
[27] A.J. Ouderkirk, P. Werner, N.L. Schultz, E. Weitz, J. Am. Chem. Soc. 105 (1983) 3354.
[28] T.A. Seder, A.J. Ouderkirk, E. Weitz, J. Chem. Phys. 85 (1986) 1977.
[29] R.J. Ryther, E. Weitz, J. Phys. Chem. 95 (1991) 9841.
[30] R.J. Ryther, E. Weitz, J. Phys. Chem. 96 (1992) 2561.
[31] P.T. Snee, C.K. Payne, K.T. Kotz, H. Yang, C.B. Harris, J. Am. Chem. Soc. 123 (2001) 2255.
[32] S.P. Church, F.W. Grevels, H. Hermann, J.M. Kelly, W.E. Klotzbücher, K. Schaffner, J. Chem. Soc., Chem. Commun. (1985) 594.
[33] F.W. Grevels, NATO ASI Ser., Ser. C. 376 (1992) 141.
[34] V. Bachler, F.W. Grevels, K. Kerpen, G. Olbrich, K. Schaffner, Organometallics 22 (2003) 1696.
[35] P. Portius, J. Yang, X.-Z. Sun, D.C. Grills, P. Matousek, A.W. Parker, M. Towrie, M.W. George, J. Am. Chem. Soc. 126 (2004) 10713.
[36] S.A. Trushin, W. Fuss, K.L. Kompa, W.E. Schmid, J. Phys. Chem. A 104 (2000) 1997.
[37] H. Ihee, J. Cao, A.H. Zewail, Angew. Chem. Int. Ed. 40 (2001) 1532.
[38] I.M. Waller, J.W. Hepburn, J. Chem. Phys. 88 (1988) 6658.
[39] B.K. Venkataraman, G. Bandukwalla, Z. Zhang, M. Vernon, J. Chem. Phys. 90 (1989) 5510.
[40] Gaussian 03, Revision C.02, M.J. Frisch, G.W. Trucks, H.B. Schlegel, G.E. Scuseria, M.A. Robb, J.R. Cheeseman, J.A. Montgomery Jr., T. Vreven, K.N. Kudin, J C. Burant, J.M. Millam, S.S. Iyengar, J. Tomasi, V. Barone, B. Mennucci, M. Cossi, G. Scalmani, N. Rega, G.A. Petersson, H. Nakatsuji, M. Hada, M. Ehara, K. Toyota, R. Fukuda, J. Hasegawa, M. Ishida, T. Nakajima, Y. Honda, O. Kitao, H. Nakai, M. Klene, X. Li, J.E. Knox, H.P. Hratchian, J.B. Cross, V. Bakken, C. Adamo, J. Jaramillo, R. Gomperts, R.E. Stratmann, O. Yazyev, A.J. Austin, R. Cammi, C. Pomelli, J.W. Ochterski, P.Y. Ayala, K. Morokuma, G.A. Voth, P. Salvador, J.J. Dannenberg, V.G. Zakrzewski, S. Dapprich, A.D. Daniels, M.C. Strain, O. Farkas, D.K. Malick, A.D. Rabuck, K. Raghavachari, J.B. Foresman, J.V. Ortiz, Q. Cui, A.G. Baboul, S. Clifford, J. Cioslowski, B.B. Stefanov, G. Liu, A. Liashenko, P. Piskorz, I. Komaromi, R.L. Martin, D.J. Fox, T. Keith, M.A. Al-Laham, C.Y. Peng, A. Nanayakkara, M. Challacombe, P.M.W. Gill, B. Johnson, W. Chen, M.W. Wong, C. Gonzalez, J.A. Pople, Gaussian, Inc., Wallingford, CT, 2004.
[41] A.D. Becke, J. Chem. Phys. 98 (1993) 5648.
[42] J.P. Perdew, Phys. Rev. B 33 (1986) 8822.
[43] J.P. Perdew, Y. Wang, Phys. Rev. B 45 (1992) 13244.
[44] (a) C. Moller, M.S. Plesset, Phys. Rev. 46 (1934) 618;
     (b) J.S. Binkley, J.A. Pople, Int. J. Quantum Chem. 9 (1975) 229.
[45] (a) C. Gonzalez, H.B. Schlegel, J. Chem. Phys. 90 (1989) 2154;
     (b) C. Gonzalez, H.B. Schlegel, J. Chem. Phys. 94 (1990) 5523.
[46] A.E. Reed, L.A. Curtiss, F. Weinhold, Chem. Rev. 88 (1988) 899.
[47] AIM2000 F.W. Biegler-Konig, J. Schonbohm, D. Bayles. J. Comput. Chem. 22 (2001) 545.
[48] (a) S. Miertus, E. Scrocco, J. Tomas, i. J. Chem. Phys. 55 (1981) 117;
     (b) S. Miertus, J. Tomasi, Chem. Phys. Lett. 65 (1982) 239;
     (c) M. Cossi, V. Barone, R. Cammi, J. Tomasi, Chem. Phys. Lett. 255 (1996) 327.
[49] M. Besora, A. Lledós, F. Maseras, Chem. Soc. Rev. 38 (2009) 957.
[50] G. Guilera, G.S. McGrady, J.W. Steed, N. Kaltsoyannis, New J. Chem. 28 (2004) 444.
[51] A.K. Saxena, N.S. Hosmane, Chem. Rev. 93 (1983) 1081.
[52] B.M. Gimarc, M. J. Am. Chem. Soc. 95 (1973) 1417.
[53] (a) A.K. Chipperfield, C.E. Housecroft, D.M. Matthews, J. Org. Chem. 384 (1990) C38;
     (b) C.E. Housecroft, D.M. Matthews, A.L. Rheingold, J. Chem. Soc., Chem. Commun. (1992) 323;
     (c) C.E. Housecroft, D.M. Matthews, A.J. Edwards, A.L. Rheingold, J. Chem. Soc., Dalton Trans. (1993) 2727.
[54] P.D. Grebenik, M.L.H. Green, M.A. Kelland, J.B. Leach, P. Mountford, G. Stringer, N.M. Walker, L.-L. Wong, J. Chem. Soc., Chem. Commun. (1988) 799.
[55] C. Ting, L. Messerle, J. Am. Chem. Soc. 111 (1989) 3449.
[56] H. Brunner, G. Gehart, W. Meier, J. Wachter, B. Wrackmeyer, B. Nuber, M.L. Ziegler, J. Org. Chem. 436 (1992) 313.
[57] R.F.W. Bader, Atoms in Molecules. A Quantum Theory. Oxford University Press, Oxford, U.K, 1990.
[58] D. Cremer, E. Kraka, Angew. Chem. 23 (1984) 627.
[59] H. Li, D. Min, S.G. Shore, W.N. Lipscomb, W. Yang, Inorg. Chem. 46 (2007) 3956.
[60] E.J.M. Hamilton, R.G. Kultyshev, B. Du, E.A. Meyers, S. Liu, C.M. Hadad, S.G. Shore, Chem. Eur. J. 12 (2006) 2571.
[61] M. Stephan, J.H. Davis Jr., X. Meng, K.J. Chase, J. Hauss, U. Zenneck, H. Pritzkow, W. Siebert, R.N. Grimes, J. Am. Chem. Soc. 114 (1992) 5214.
[62] C.A. Plumb, P.J. Carroll, L.G. Sneddon, Organometallics 11 (1992) 1672.
[63] L.E. Roy, P.J. Hay, R.L. Martin, J. Chem. Theory Comput. 4 (2008) 1029.
[64] H.W. Smith, W.N. Lipscomb, J. Chem. Phys. 43 (1965) 1060.